NUCL SCI TECH (2017) 28:178
https://doi.org/10.1007/s41365-017-0330-8

Effect of thermal exposure time on tellurium-induced embrittlement of Ni–16Mo–7Cr–4Fe alloy

Xiang-Wei Chu[2] · **Hong-Wei Cheng**[3] · **Cai-Tao Fu**[1,2,3] · **Bin Leng**[1] ·
Yan-Yan Jia[1] · **Fang Liu**[2] · **Zhi-Jun Li**[1]

Received: 17 October 2016 / Revised: 20 March 2017 / Accepted: 1 April 2017 / Published online: 21 November 2017

Abstract The embrittlement of nickel-based structural alloys by fission-produced tellurium (Te) is a major challenge for molten salt reactors (MSR). In this study, the effects of thermal exposure time on tellurium diffusion in a candidate MSR structural alloy (Ni–16Mo–7Cr–4Fe) and the consequent mechanical property degradation of the alloy were investigated through surrogate diffusion experiments at 700 °C. The results show that some tellurium reacted with the alloy to form tellurides on the surface, while some tellurium diffused into the alloy along grain boundaries. Ni_3Te_2 and CrTe were the most stable reaction products at the tested temperature, and the formation of CrTe on the surface induced the Cr depletion at grain boundaries of the alloy. The diffusion depth of Te increased gradually with thermal exposure time, and the diffusion rate kept stable within the test duration of up to 3000 h. The Te diffusion in the alloy caused the embrittlement of grain boundaries, inducing crack formation and strength degradation in tensile test at room temperature.

Keywords Tellurium · Grain boundary · Embrittlement · Intergranular cracking · Nickel-based alloy · Molten salt reactor

1 Introduction

Nuclear power is one of the best choices to meet future energy demands due to its advantages in fuel economy, reliability, and carbon emission reduction. Molten salt reactor (MSR) is a promising candidate for next-generation reactors and is the only liquid-fueled reactor selected in the Generation IV reactor concepts [1]. By dissolving nuclear fuel in molten fluoride salts, MSR is advantageous in its high negative temperature coefficient of reactivity, low vapor pressure, water free cooling, and passive safety [2–4]. However, this also brings a unique problem that certain fission products will dissolve in the fuel salt and transport through the reactor vessel and primary loop, causing degradation of alloy components during service [5].

Ni–16Mo–7Cr–4Fe alloy is chosen as the main structural material for MSR due to its excellent molten salt corrosion resistance and good high temperature strength [6], but it is reportedly vulnerable to tellurium (Te), a fission product in fuel salt [7]. Studies show that Te atoms prefer to diffuse along the grain boundaries (GBs) in the alloy [8, 9]. The GB diffusion of Te induces grain boundary embrittlement and causes surface cracks in the

---

This work was supported by the National key research and development program of China (No. 2016YFB0700404), the National Natural Science Foundation of China (Nos. 51371188, 51671122, 51671154, 51601213, 51501216), the Strategic Priority Research Program of the Chinese Academy of Sciences (No. XDA02004210), the Shanghai Sailing Program (No. 16YF1414300) and the Talent development fund of Shanghai (No. 201650).

✉ Fang Liu
liufang@usst.edu.cn

✉ Zhi-Jun Li
lizhijun@sinap.ac.cn

[1] Shanghai Institute of Applied Physics, Chinese Academy of Science, Jiading Campus, Shanghai 201800, China

[2] School of Materials Science and Engineering, University of Shanghai for Science and Technology, Shanghai 200093, China

[3] National Center for Electron Microscopy in Beijing, Tsinghua University, Beijing 100084, China

alloy components under certain stresses, which threaten the safety of MSR. According to experimental results, Te embrittlement of nickel-based alloys is affected by Te concentration [10], temperature [11], and redox potential of molten salts [12]. However, the thermal exposure time for Te diffusion in the experiments is relevantly short (less than 500 h), whereas the designed service life of the alloy in MSR is usually decades. Therefore, the effects of thermal exposure time on Te embrittlement behavior of Ni–16Mo–7Cr–4Fe were investigated in this study, for a better estimation of the long term service behavior of the alloy.

2 Experimental procedures

The ingot of Ni–16Mo–7Cr–4Fe (GH3535, made in China by vacuum-inducing melting, with its chemical composition showing in Table 1) was remelted by vacuum consumable arc remelting (VAR), to improve chemical homogeneity. Sample rods of Φ16 mm were treated at 1177 °C for 45 min followed by water-quenching. The bulk specimens (15 mm × 10 mm × 1 mm) and dog bone-shaped plate tensile specimens (with a thickness of 2 mm and a gage length of 20 mm) were cut from the alloy rods by electrospark wire-electrode cutting. Finally, all specimens were polished using metallographic SiC paper to 1200 grid and ultrasonically cleaned in acetone for surface finishing.

Diffusion experiment was done by sealing bulk and tensile specimens along with Te powders (99.99% in purity) in vacuum quartz ampoules and exposing them at 700 °C in a muffle furnace. The quantity of Te powders in each ampoule was determined by the total surface area of the specimens sealed, keeping the proportion of Te mass to specimen area at approximately 1.0 mg/cm^2. This value corresponds with the fluence of Te accumulated on the surface of the container wall in a MSR primary circuit after 5 years of operation for a single-fluid 2240 MWt molten salt breeder reactor [7, 12]. The ampoules were taken out from the furnace after thermal exposure of 100–3000 h and were allowed to cool for determining the effect of exposure time. The controls were thermal exposed at the same condition in vacuum ampoules without Te.

X-ray diffraction (XRD, DX2700) system was used to identify surface reaction products of the specimens, using Cu-K X-ray at accelerating voltage of 40 kV and beam current of 40 mA. Electron probe micro-analyzer (Shimadzu EPMA-1720H) was employed to do elemental mapping of the specimens, at acceleration voltage of 25 kV and beam current of 10 nA. Tensile properties of the specimens were measured at room temperature on a Zwick/Roell Z100 universal tensile testing machine, with cross-head speed setting at 3.55 mm/min. Optical microscope (OM ZEISS XAIO) was employed to observe micro-cracks on the gage of the tensile-tested specimens.

Table 1 Chemical composition of test alloy (wt%)

Ni	Mo	Cr	Fe	Mn	Si	Al	C	Nb	*P*
Balance	15.9	6.88	4.1	0.49	1.01	0.88	0.05	0.01	0.003

3 Results and discussion

During the thermal exposure, Te powders were vaporized at 700 °C and reacted with the alloy. Figure 1 shows XRD spectra of the Te-defused specimens. Various surface reaction products were formed on the specimen. $Ni_3Te_{2.07}$, Ni_3Te_2, CrTe, and trace amount of $MoTe_2$ were identified on specimens exposed for 100 and 300 h. At 3000 h, the peak intensities of Ni_3Te_2 and CrTe increased apparently, but $MoTe_2$ and $Ni_3Te_{2.07}$ were no longer detected. As the exposure time increased, $Ni_3Te_{2.07}$, an unstable telluride, could be converted into Ni_3Te_2, a relatively stable phase of nickel telluride [13]. As a telluride being more stable than $MoTe_2$ at 700 °C [11], CrTe gradually formed on the surface during the exposure through the GB diffusion of Cr outward, as shown in Fig. 2.

Te and Cr distributions obtained by EPMA on the specimen cross sections are shown in Fig. 2. In Fig. 2b, d, f, h, Te gradually diffused into the alloy along GBs, whereas In Fig. 2a, c, e, g, Cr diffused along GBs but toward the opposite direction. However, Cr diffusion did not occur in the specimen for thermal exposure of 3000 h without Te (Fig. 2k). The Te diffusion depth and Cr depletion depth increased constantly with exposure time.

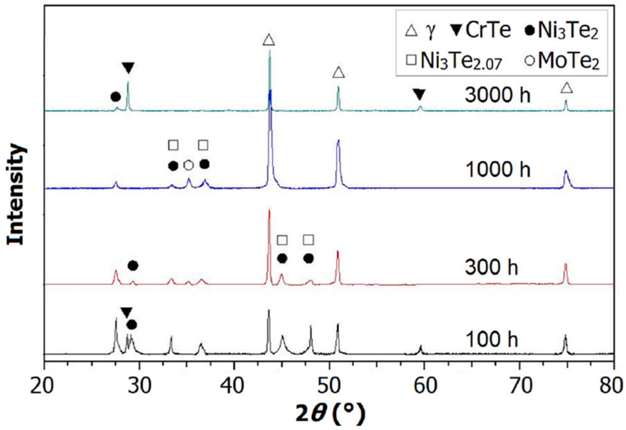

Fig. 1 (Color online) XRD spectra of samples thermal exposed at 700 °C for different times in the Te-containing environment

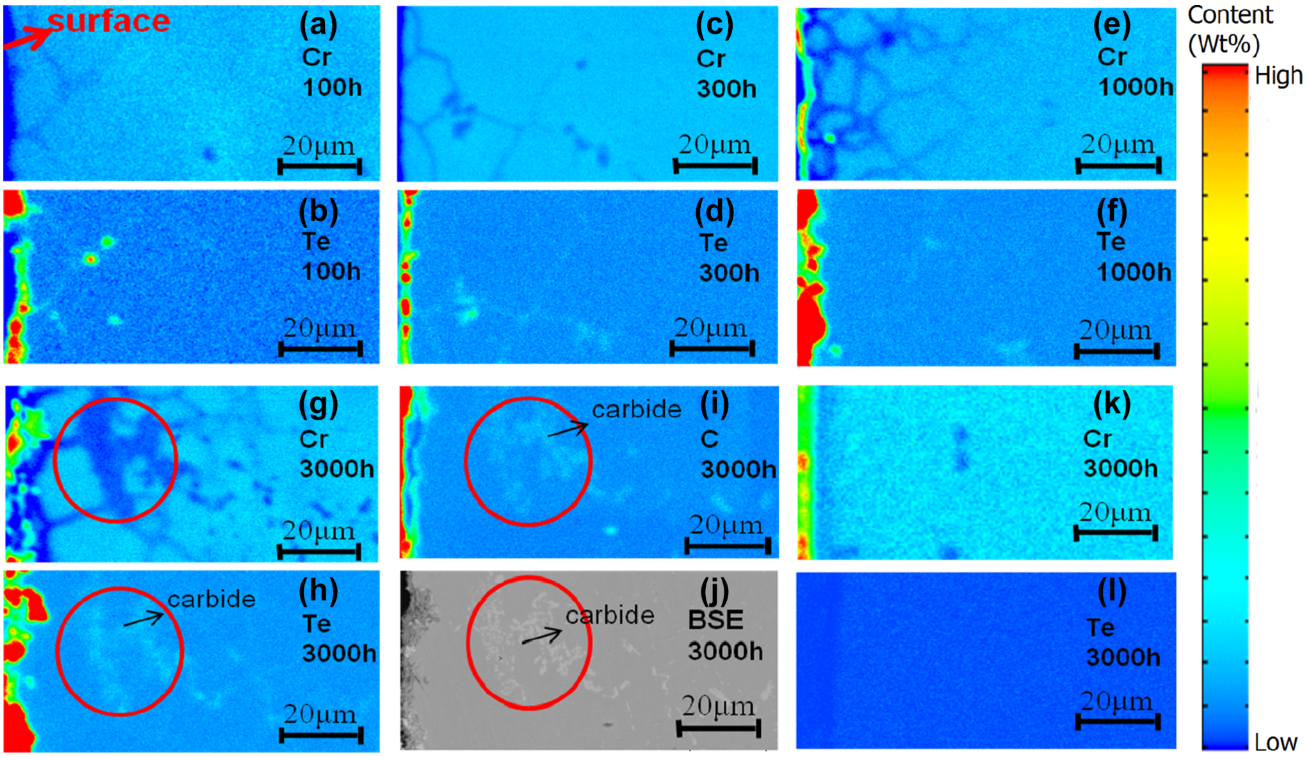

Fig. 2 (Color online) EPMA elemental mapping of Cr and Te in specimens exposed at 700 °C in Te-containing environment for 100–3000 h (**a**–**h**), carbon distribution (**i** and **j**) in the 3000-h exposure specimens, and Cr and Te mapping (**k** and **l**) in the control (700 °C, 3000 h without Te)

Intergranular diffusion of Te was not seen even after 3000 h of exposure, indicating that the lattice diffusivity of Te in Ni–16Mo–7Cr–4Fe is far lower than the GB diffusivity. The Cr depletion is due to the formation of CrTe on the specimen surface, from the XRD results.

For studying mechanical property degradation of the alloy after Te diffusion, room-temperature tensile tests were performed on the specimens. Figure 3 shows cross-sectional morphologies of the Te-exposed and tensile-tested specimens (left), compared with the controls (right). Extensive cracks were observed on surface of the Te-exposed specimens. The number and width of the cracks increased with the exposure time, and some small grains spalled off in the near surface region. The cracking became severer with the increase of exposure time. On the contrary, no cracks were found in the controls, even after 3000 h of exposure. Quantitatively the degree of cracking in the Te-exposed specimens can be described by the *K* value, defined as crack number per cm multiplied by an average depth in micrometers. It was first utilized by Oak Ridge National Laboratory [13] for the Te effect on cracking sensitivity of the alloy, and later by Kurchatov Institute [9, 14]. In this work, *K* values of the Te-exposed specimens for 100–3000 h are 76 pc $\mathrm{cm}^{-1} \times 52.7$ μm, 85 pc $\mathrm{cm}^{-1} \times 66$ μm, 78.4 pc $\mathrm{cm}^{-1} \times 94.8$ μm, and 85.2 pc $\mathrm{cm}^{-1} \times 135$ μm, respectively. The crack depth increased obviously with the exposure time.

Fracture morphology of room-temperature tensile-tested specimens are shown in Fig. 4. The tellurium diffusion regions exhibit typical intergranular brittle fracture features, while the regions where tellurium barely diffused show a ductile fracture mode. The measured depths of the intergranular fracture zones in Fig. 4 agree well with the Te diffusion depth measured by EPMA mapping. Therefore, for better statistics, 10 measurements of intergranular fracture zone depths from different locations are considered as the effective diffusion depth. The results are given in Table 2. The effective diffusion coefficient D can be calculated $x = (Dt)^{1/2}$, where x is effective diffusion depth and t is thermal exposure time. From Table 2, we found that x was in direct proportion to $t^{1/2}$. Through a linear fitting of x versus $t^{1/2}$ (Fig. 5), the effective diffusion coefficient of Te in Ni–16Mo–7Cr–4Fe at 700 °C was $D = 1.68 \times 10^{-11}$ cm^2/s. It can be seen that diffusion depths fit well with exposure times, indicating that the diffusion rate in 3000 h maintains quite stable.

Surface cracking can consequently result in the degradation of tensile properties. The exposure time effect on room-temperature tensile properties of the specimens is shown in Fig. 6. The ultimate tensile strength (UTS) of Te-exposed specimens decreased drastically with increasing

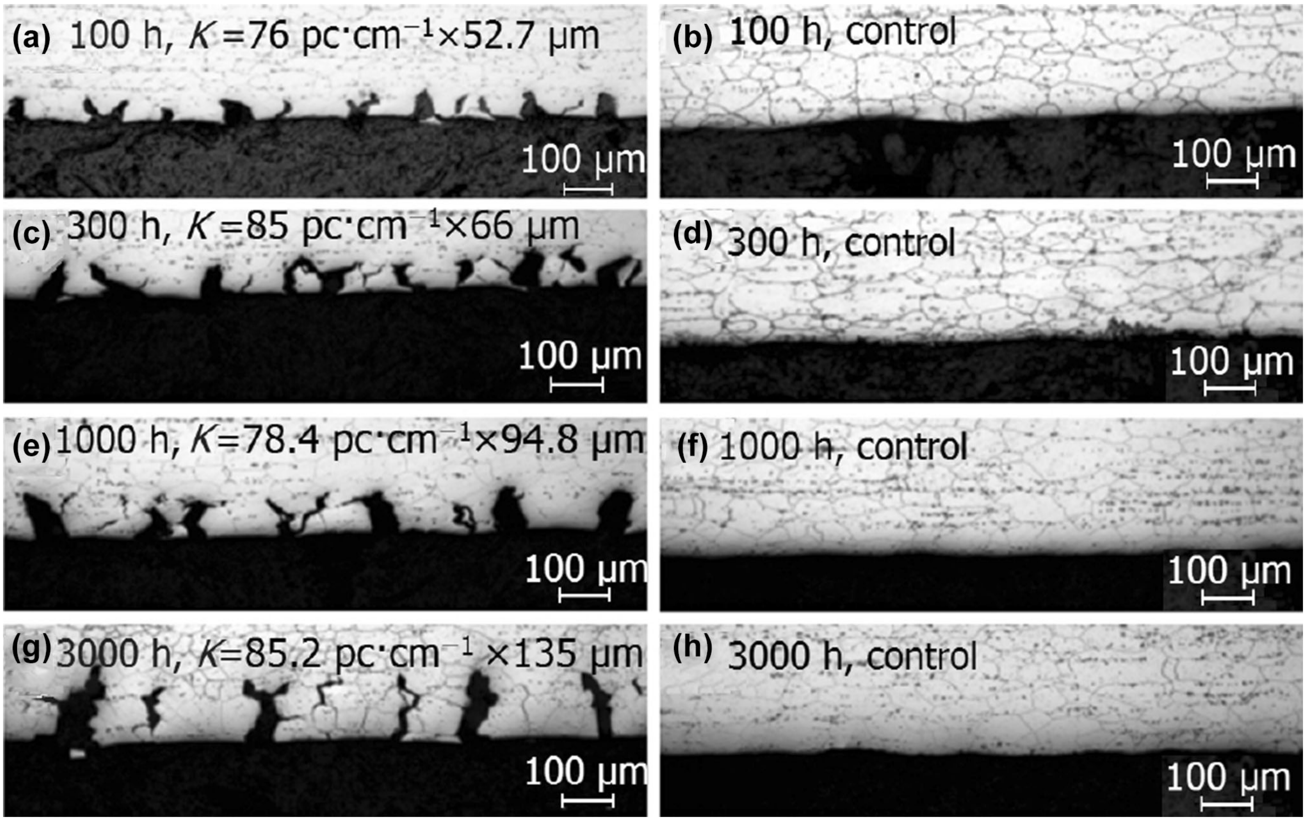

Fig. 3 Near-surface cross-sectional images of the RT tensile-tested specimens of different Te exposure hours, compared with the controls

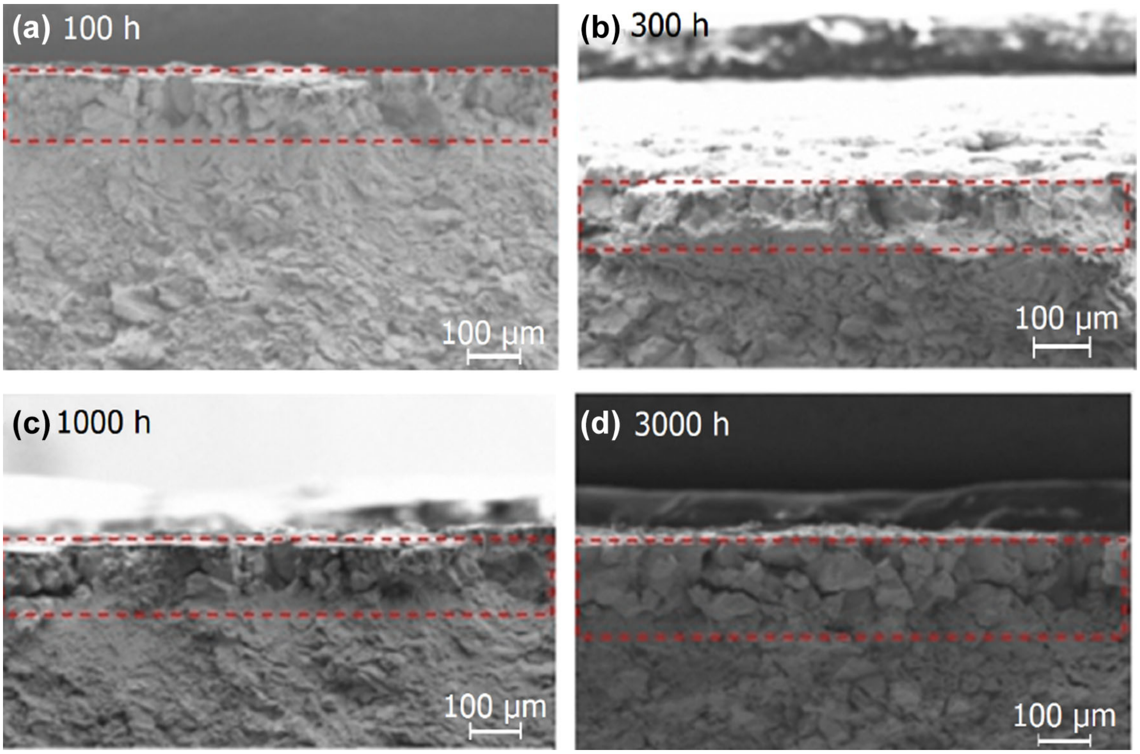

Fig. 4 (Color online) SEM fracture morphology of room-temperature tensile-tested specimens exposed in Te-containing environment for 100–3000 h

Table 2 Depth of Te diffusion at 700 °C for different hours

Exposure time (h)	100	300	1000	3000
Diffusion depth (μm)	53 ± 3	63 ± 5	79 ± 4	135 ± 9

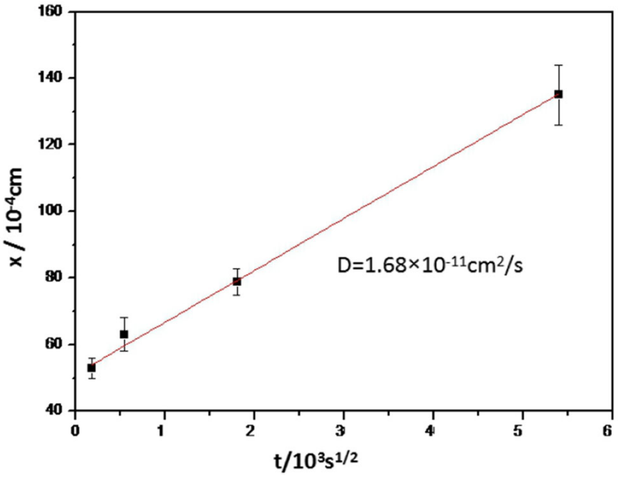

Fig. 5 Linear fitting for calculating the effective diffusion coefficient of Te at 700 °C

exposure time, whereas UTS of the controls remained unchanged basically. After 100 and 3000 h of exposure, UTS of the Te-exposed specimens was 775 and 650 MPa, declined by 8.3 and 22.6%, respectively, compared to those of the controls. The elongation (EL) of the Te-exposed specimens and the controls slightly decreased with increasing exposure time, but ELs of the Te-exposed specimens were lower than those of the controls at all the exposure hours.

Simulation studies predicted that the Te diffusion causes GB embrittlement of nickel-based alloys. Všianska and Šob [15] proposed by the first-principles study that Te could draw charge from adjacent nickel atoms and reduce the strength of nearby Ni–Ni bonds, and the GB diffusion of Te could cause decohesion and embrittlement of GBs. Liu et al. [9] testified by the first principles that Te atoms occupying the site of Ni atoms would cause elongation of bond length and bond strength of the adjacent Ni atoms, inducing GB expansion and weakening the Ni–Ni bonds. It is clear that the change of GB chemical structure has vital effect on strength of the GBs, and the weakened GBs can act as preferential sites for the crack formation in room-temperature tensile tests. In this study, Te element diffused into alloy along GBs, and the diffusion depth increased with the thermal exposure time. And the intergranular embrittlement and cracking increased with the diffusion depth. Accordingly, with increasing exposure time, the tensile properties degraded significantly and the cracking sensitivity factor *K* increased greatly.

4 Conclusion

When Ni–16Mo–7Cr–4Fe specimens were thermally exposed together with Te vapor at 700 °C, a reaction layer contained various tellurides which formed on the surface of the alloy. With the increase in exposure time, contents of Ni_3Te_2 and CrTe increased, whereas other tellurides diminished, indicating that these two tellurides are the most stable at this temperature. The formation of CrTe on the surface induced the Cr depletion at grain boundaries of the alloy.

Te diffused in Ni–16Mo–7Cr–4Fe along the grain boundaries, and the diffusion depth gradually increased with the increasing thermal exposure time up to 3000 h. Te diffusion rate kept stable within the tested exposure times, and effective diffusivity were calculated to be $D = 1.68 \times 10^{-11}$ cm²/s.

The grain boundary diffusion of Te caused the embrittlement of the grain boundaries of Ni–16Mo–7Cr–4Fe, and hence cracks formed on the diffusion zone after room-temperature tensile tests. Both the cracking sensitivity and tensile properties degradation of the alloy increased with the extended thermal exposure time.

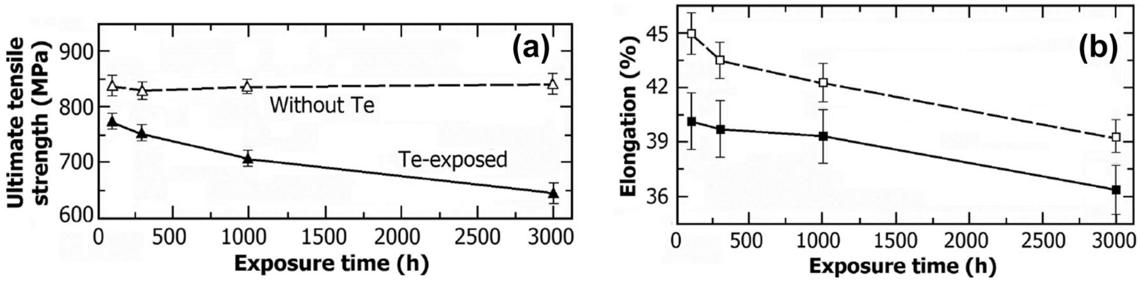

Fig. 6 Changes in tensile properties of the specimens after different thermal exposure times in environments with and without Te: **a** ultimate tensile strength (UTS); **b** elongation (EL)

References

1. T. Abram, S. Ion, Generation-IV nuclear power: a review of the state of the science. Energy Policy **36**, 4323–4330 (2008). https://doi.org/10.1016/j.enpol.2008.09.059
2. X.L. Li, S. He, X. Zhou et al., Improvement of the oxidation resistance of Ni–16Mo–7Cr–4Fe nickel-based superalloy by yttrium microalloying. Nucl. Tech. **26**, 030202 (2015). https://doi.org/10.13538/j1001-8042/nst26.030201. **(in Chinese)**
3. J. Tian, X.B. Xia, C. Peng et al., Impact analysis of criticality safety for 10-MWt solid thorium-based molten salt reactor spent nuclear fuel storage system. Nucl. Sci. Technol. **5**, 86–91 (2015). https://doi.org/10.11889/j.0253-3219.2015.hjs.38.050602
4. J. Qiu, Y. Zou, G.J. Yu et al., Speciation study of chromium corrosion product in molten LiF–NaF–KF salt. Nucl. Sci. Technol. **26**, 060602 (2015). https://doi.org/10.13538/j.1001-8042/nst.26.060602
5. H.E. McCoy, B. McNabb, *Intergranular Cracking of INOR-8 in the MSRE* (Oak Ridge National Laboratory, Oak Ridge, 1972). **(ORNL-4829)**
6. P.K. Vijayan, A. Basak, I.V. Dulera et al., Conceptual design of Indian molten salt breeder reactor. Pramana **85**, 539–554 (2015). https://doi.org/10.1007/s12043-015-1070-0
7. J.R. Keiser, *Status of Tellurium–Hastelloy N Studies in Molten Fluoride Salts* (Oak Ridge National Laboratory, Oak Ridge, 1977), pp. 1–2. **(ORNL-TM-6002)**
8. Y.Y. Jia, H.W. Cheng, J. Qiu et al., Effect of temperature on diffusion behavior of Te into nickel. J. Nucl. Mater. **441**, 372–379 (2013). https://doi.org/10.1016/j.jnucmat.2013.06.025
9. W. Liu, H. Han, C. Ren et al., First-principles study of intergranular embrittlement induced by Te in the Ni Σ 5 grain boundary. Comput. Mater. Sci. **88**, 22–27 (2014). https://doi.org/10.1016/j.commatsci.2014.02.038
10. H. Cheng, F. Han, Y. Jia et al., Effects of Te on intergranular embrittlement of a Ni–16Mo–7Cr alloy. J. Nucl. Mater. **461**, 122–128 (2015). https://doi.org/10.1016/j.jnucmat.2015.01.049
11. H. Cheng, Z. Li, B. Leng et al., Intergranular diffusion and embrittlement of a Ni–16Mo–7Cr alloy in Te vapor environment. J. Nucl. Mater. **467**, 341–348 (2015). https://doi.org/10.1016/j.jnucmat.2015.09.053
12. V. Ignatiev, A. Surenkov, I. Gnidoy et al., Intergranular tellurium cracking of nickel-based alloys in molten Li, Be, Th, U/F salt mixture. J. Nucl. Mater. **440**, 243–249 (2013). https://doi.org/10.1016/j.jnucmat.2013.05.001
13. J. Barstad, G. Fredrik, R. Erling et al., On the tellurides of nickel. Acta Chenica Scand. **20**, 2865–2879 (1966). https://doi.org/10.3891/acta.chem.scand.20-2865
14. V. Ignatiev, A. Surenkov, Alloys compatibility in molten salt fluorides: Kurchatov Institute related experience. J. Nucl. Mater. **441**, 592–603 (2013). https://doi.org/10.1016/j.jnucmat.2013.05.007
15. M. Všianská, M. Šob, The effect of segregated sp-impurities on grain-boundary and surface structure, magnetism and embrittlement in nickel. Prog. Mater. Sci. **56**, 817–840 (2011). https://doi.org/10.1016/j.pmatsci.2011.01.008